3D HELIOSPHERIC RECONSTRUCTIONS FROM THE SECCHI WHITE LIGHT CORONAGRAPHS ONBOARD STEREO: RESULTS FROM THE EARLY RECONSTRUCTIONS

J.W. Cook, J.S. Newmark (Naval Research Laboratory), P.A. Reiser, P.C. Crane (Interferometrics), A. Yahil, T. Gosnell, and R. Puetter (Pixon LLC)

The twin STEREO spacecraft will carry onboard the SECCHI (Sun-Earth Connection Coronal and Heliospheric Investigation) experiment, consisting of an EUVI disk imager and three white light coronagraphs on each spacecraft. At NRL we are investigating the tomographic electron density reconstructions, and their limitations, which are achievable from just two viewpoints using the coronagraph observations. We employ the PIXON technique for reconstruction. In this presentation we discuss results from early reconstructions.

We have started with simple geometrical volumes of constant 1×10^{8} cm^{-3} electron number density: cylinders (toy coronal polar plumes), and hemispherical shells with a main axis along a line to Sun center (toy coronal mass ejections). We have results for all model problems with 64×64×64 resolution volumes, and selected problems with 128×128×128 resolution. Our model coronagraph observes to 15 $R_{\odot}$, with an occulter extending to 1.3 $R_{\odot}$. We render from the starting known electron density distribution within a 3D volume (the input IMAGE) a synthetic white light input DATA 2D picture, in radial and tangential polarizations. We use two viewpoints in the ecliptic plane, at 0° (behind B spacecraft) and 37°(ahead A spacecraft), appropriate for early in the STEREO mission, or three viewpoints, at -37° (B), 0° (Earth), and 37° (A). From these input synthetic observations, our PIXON technique produces an electron density reconstruction (3D output IMAGE), using the fewest PIXON elements, that renders 2D output DATA pictures which best agree with the 2D input DATA pictures. We discuss the following test problems, illustrating the degree of agreement of the PIXON output IMAGE reconstructions with the known starting input IMAGE model electron density distributions, and of the rendered input and output DATA pictures. We are particularly interested in the limitations present when only two viewpoints are available. The test problems are:

1. Plumes, finite geometry, 2 viewpoints, polarization
2. Plumes, *infinite* geometry, 2 viewpoints, polarization
3. Plumes, finite geometry, *3 viewpoints*, polarization
4. Plumes, finite geometry, 2 viewpoints, *brightness*
5. CME, finite geometry, 2 viewpoints, polarization
6. CME, *infinite* geometry, 2 viewpoints, polarization
7. CME, finite geometry, *3 viewpoints*, polarization
8. CME, finite geometry, 2 viewpoints, *brightness*

9-13. CME, finite geometry, 2 viewpoints, polarization, *CME at angles to the plane of the sky of 60°, 45°, 0°, -45°, and -60°.* We illustrate that reconstructions are possible for structures far from the plane of the sky. The fundamental consideration is the signal-to-noise level of the input DATA observations used. (In interpreting our results, to express DATA intensities in terms of B/B_O, for our choice of problem numerical values, $B_O = 5.6\times10^{20}$ ph cm^{-2} s^{-1} sr^{-1}. Our test objects are unrealistically bright, both from the assumed electron density and from the choice of solar spectral parameters employed. We are still learning!)

We have for each test problem a group of diagnostic figures to evaluate the reconstruction. We illustrate below selected diagnostic figures for test problems 1 and 5, the standard plumes and CME problems, at 128×128×128 resolution. For problems 1 and 5 we show:

DATA rendered from the input and PIXON output IMAGE 3D electron density distributions. Look for differences;
The above rendered synthetic DATA placed in the model CCD field-of-view;

Two pictorial quantitative representations of the difference between the input and PIXON output DATA;
A visualization of the input and PIXON output IMAGE 3D electron density distributions along four representative viewpoints. Notice the differences viewed from the +z axis, where the PIXON reconstruction is least constrained by the input DATA;
Two histogram representations of the quantitative difference between the input and PIXON output DATA;
Two histogram representations of the quantitative difference between the input and PIXON output IMAGE 3D electron density distributions.

We have with us the diagnostic figures for all of the problems, and will use them in individual discussions about the results from our series of test problems. We compare reconstructions using realistic, finite geometry lines-of-sight vs. infinite geometry with all lines-of-sight parallel (Sun at infinity); reconstructions using two viewpoints vs. an extra third viewpoint; and reconstructions using tangential and radial polarizations vs. brightness alone. With only two viewpoints it is possible to produce "shadow" reconstructed artifacts of the features which were present in the starting model volume, via the symmetry of the two viewpoint angles. These artifacts are partly removed with the addition of the third viewpoint to the reconstruction.

We will make selected reconstructions available to the STEREO community as test problems. We solicit for the SECCHI effort the contributions of outside researchers to this very difficult problem. The test problems, with information describing the test data and model parameters used, can be found at http://stereo.nrl.navy.mil by following the “3D R & V” link.

This work is supported by NASA under S-13631-Y, and by the Office of Naval Research. The SECCHI experiment is an international collaboration led by the Naval Research Laboratory.

Figure 1. Rendered DATA

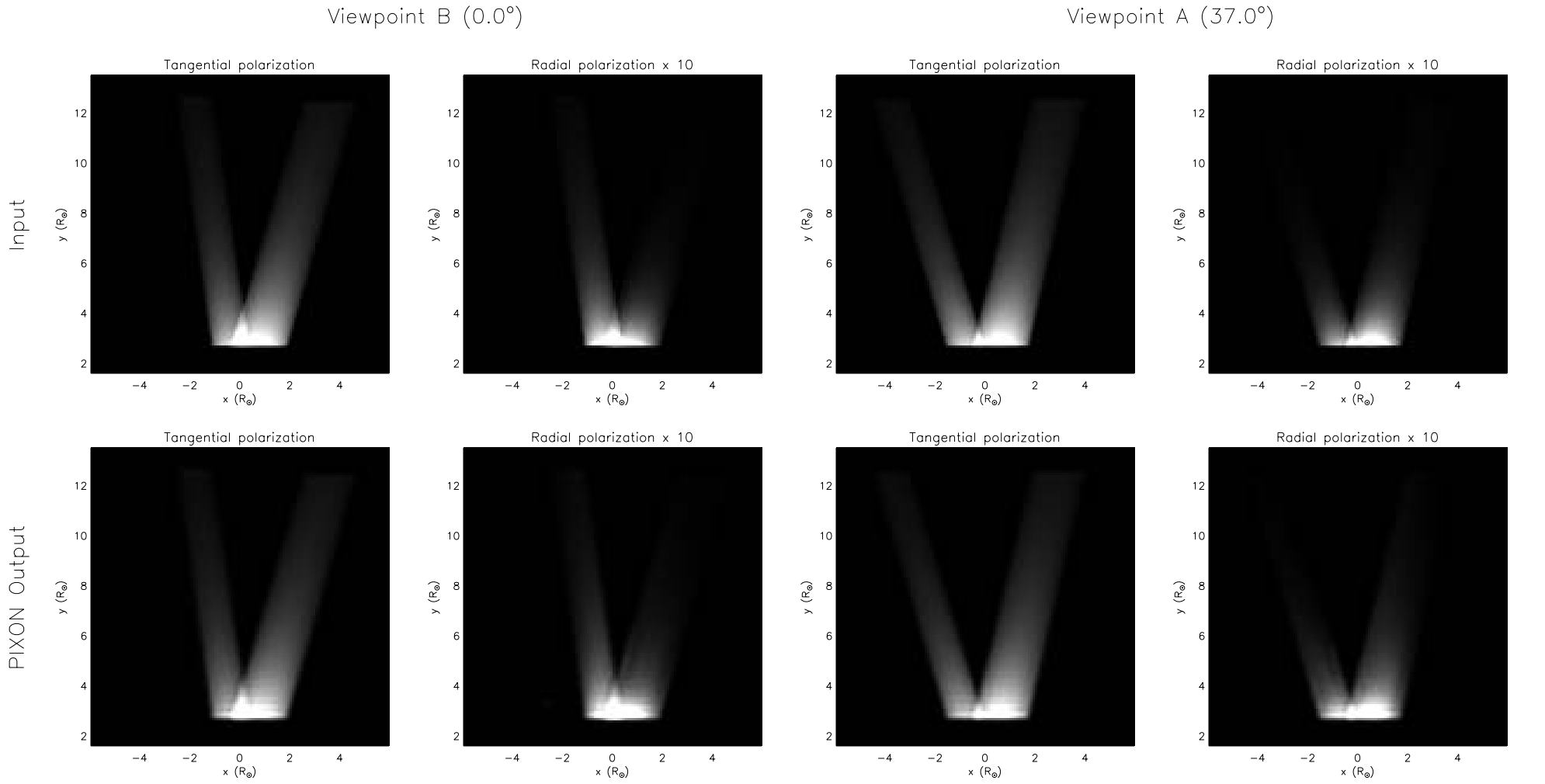

out_paris__128_01_03b

Figure 3. Synthetic CCD DATA

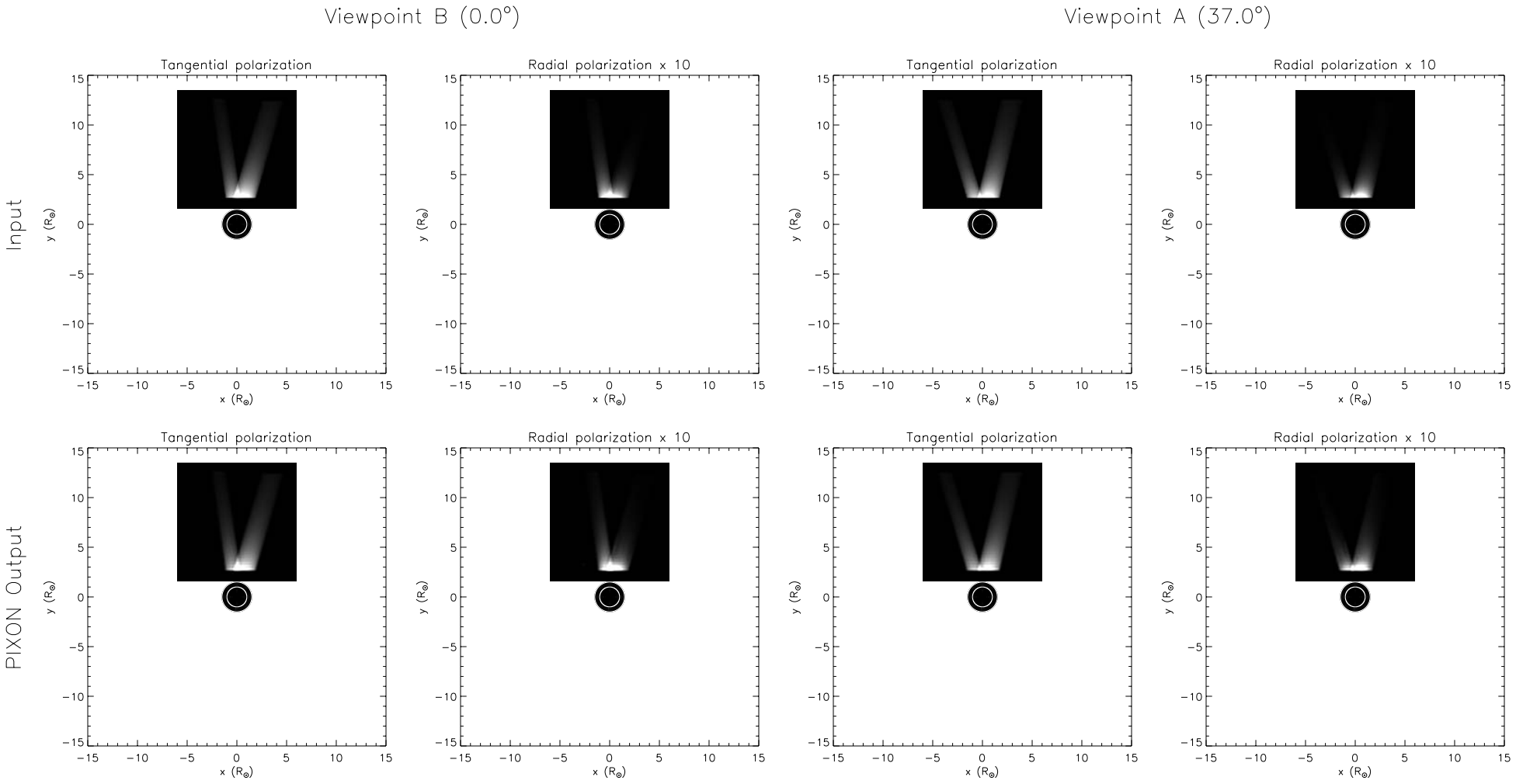

Linear [0, 2.50e+16] photons sec^{-1} cm^{-2} sr^{-1}

out_paris__128_01_03b

Figure 4. Residuals of Rendered DATA

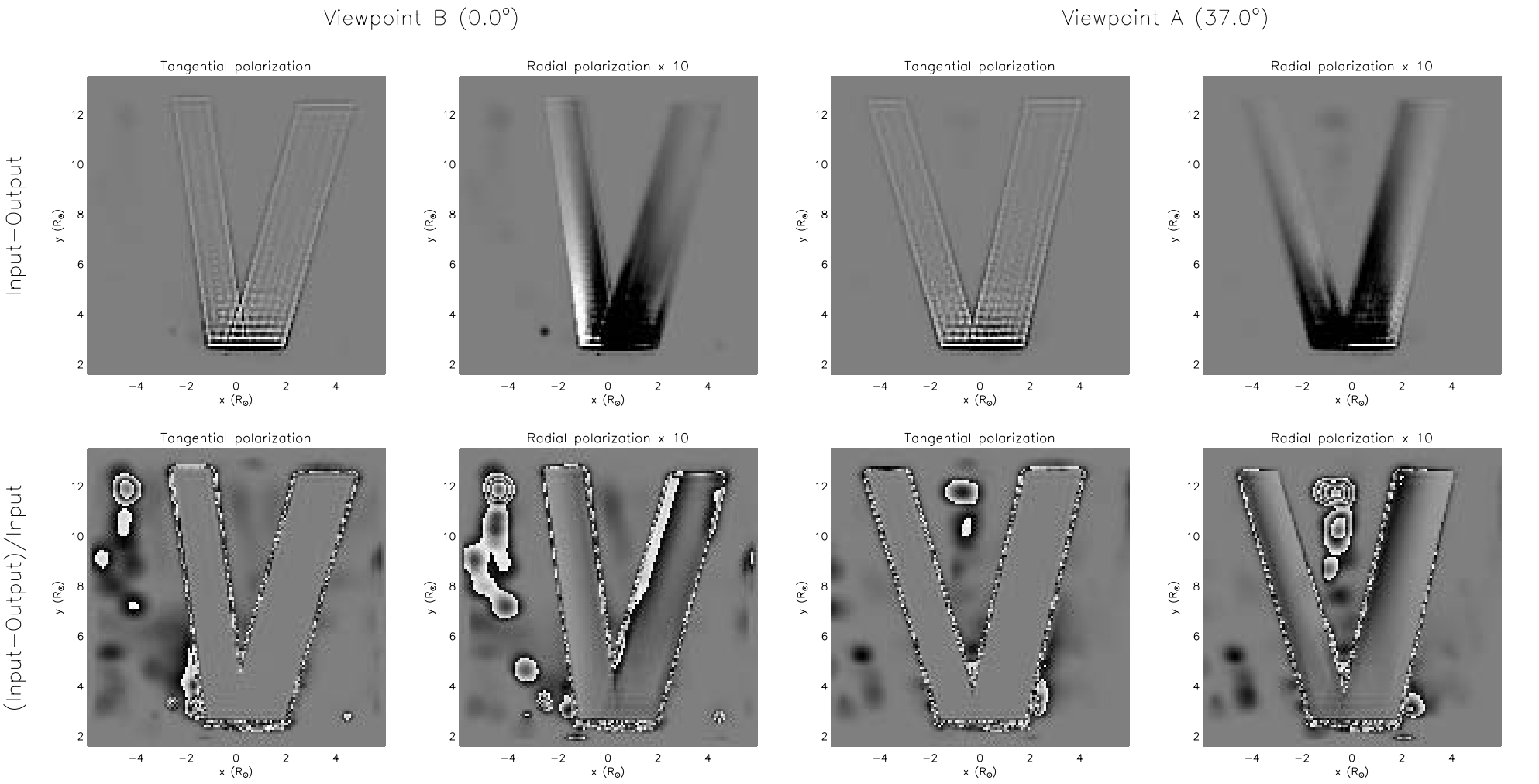

Linear [−1.25e+15, 1.25e+15] photons sec^{-1} cm^{-2} sr^{-1}, No threshold

Fractional error [−2.00, 2.00], Input threshold: 1.25e+13 photons sec^{-1} cm^{-2} sr^{-1}

out_paris__128_01_03b

Figure 5. IMAGEs Visualized from Principal Viewpoints

Column Density, Infinite Geometry

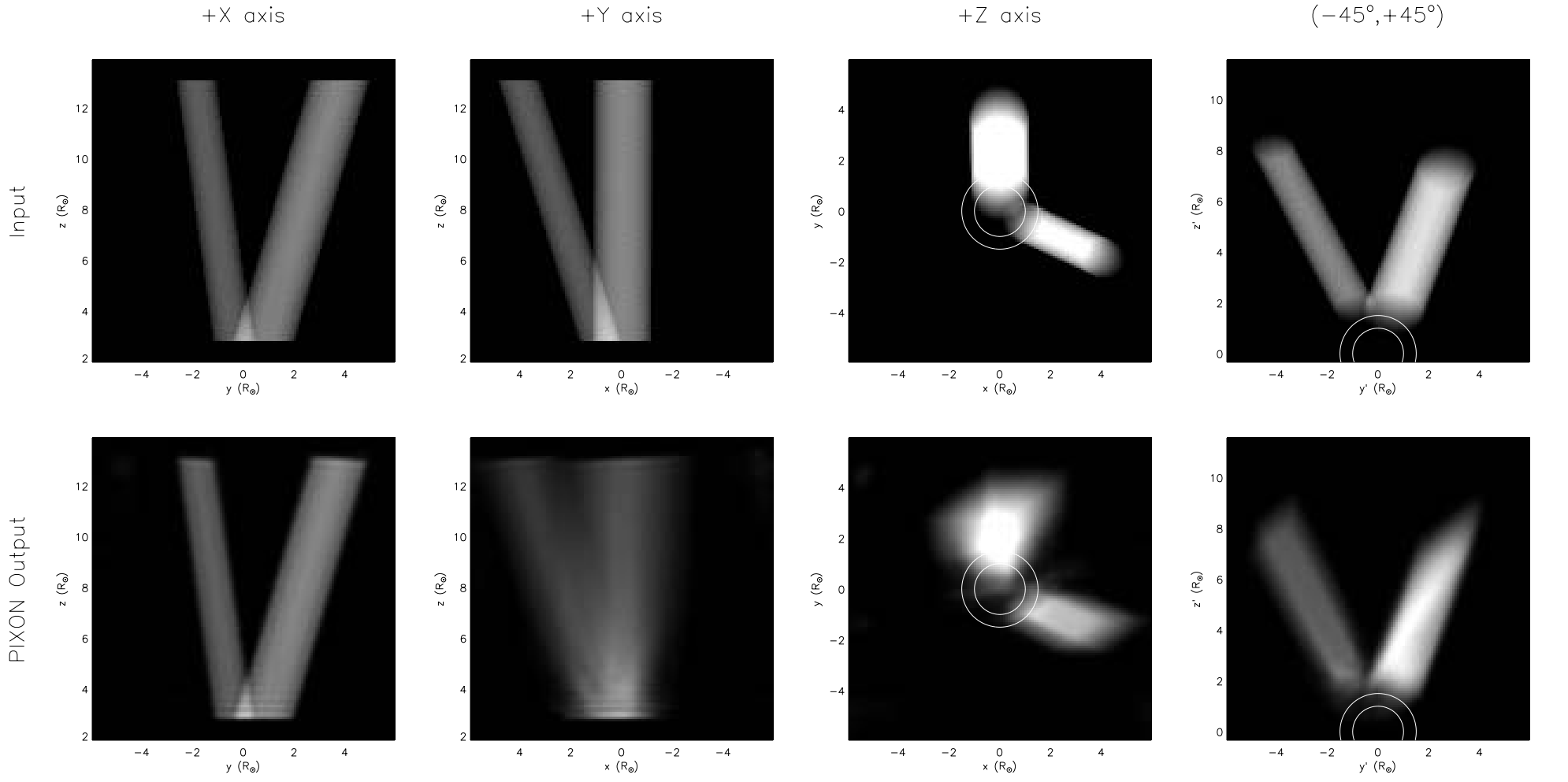

Linear [0, 3.00e+19] electrons cm^{-2}

out_paris__128_01_03b

Figure 7. Histograms of Rendered DATA Above Threshold

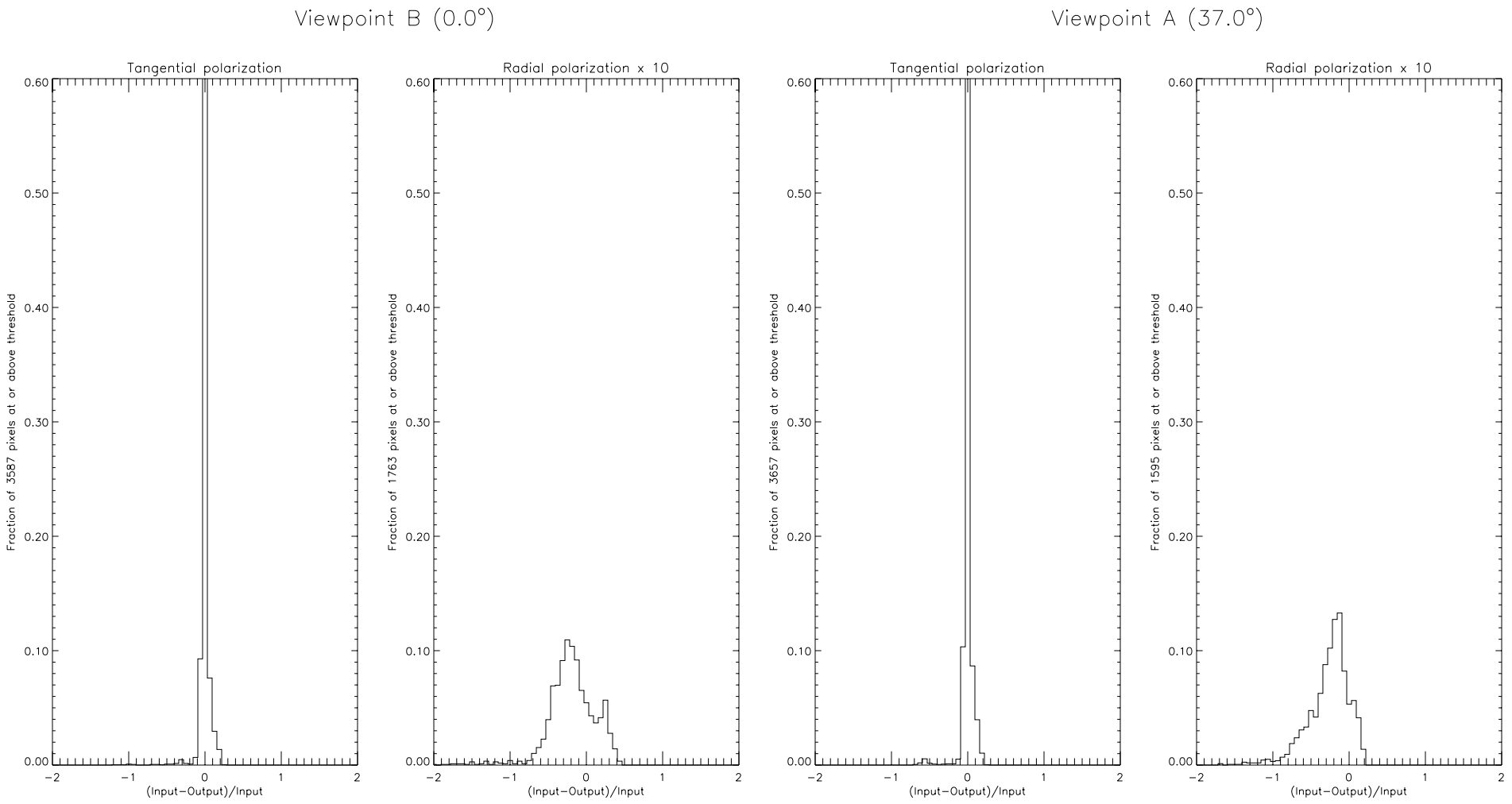

Input Threshold: 1.25e+15 photons sec^{-1} cm^{-2} sr^{-1}

out_paris__128_01_03b

Figure 8. Histograms of IMAGES

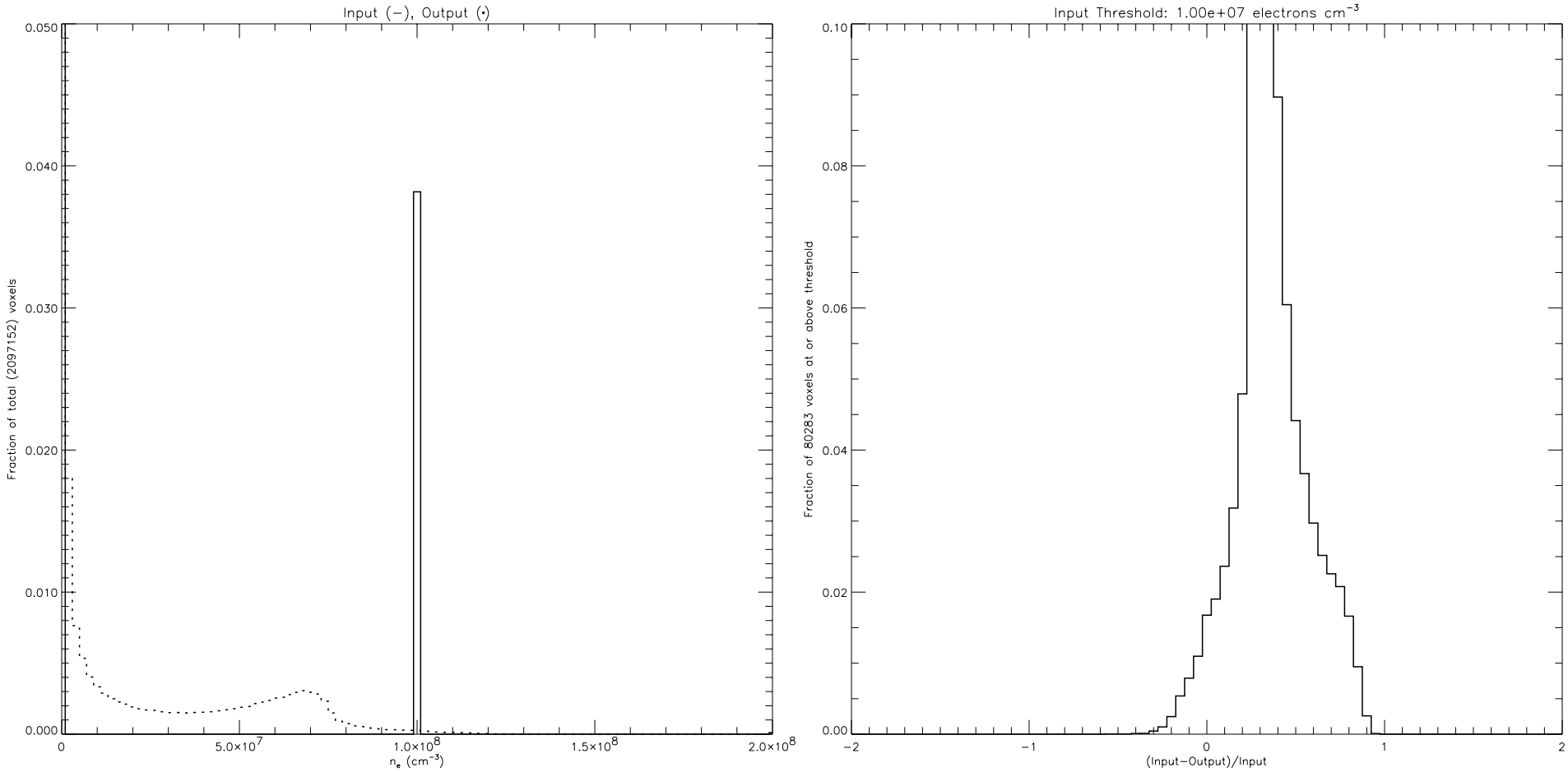

out_paris__128_01_03b

Figure 1. Rendered DATA

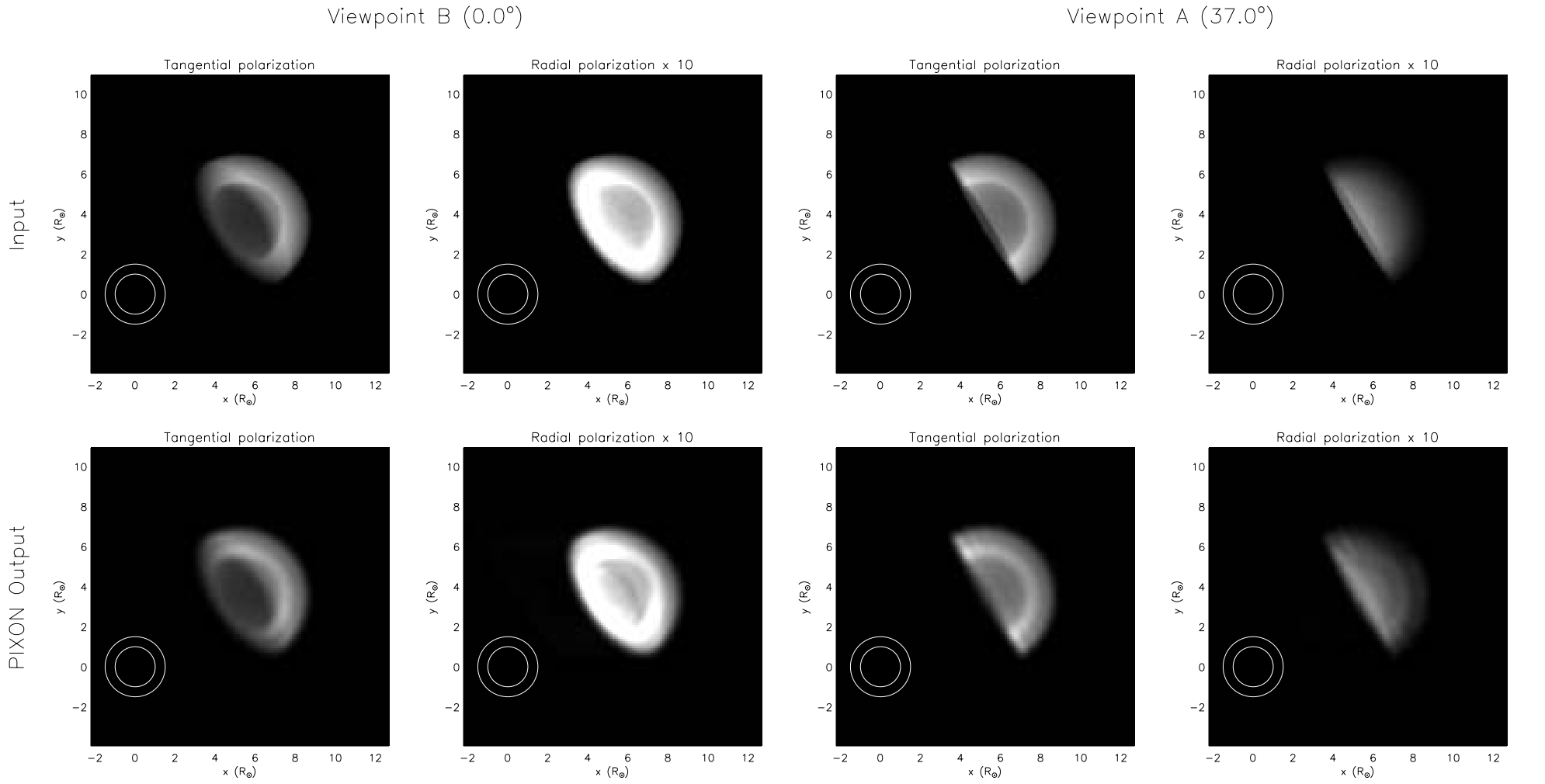

out_paris__128_05_03b

Figure 4. Residuals of Rendered DATA

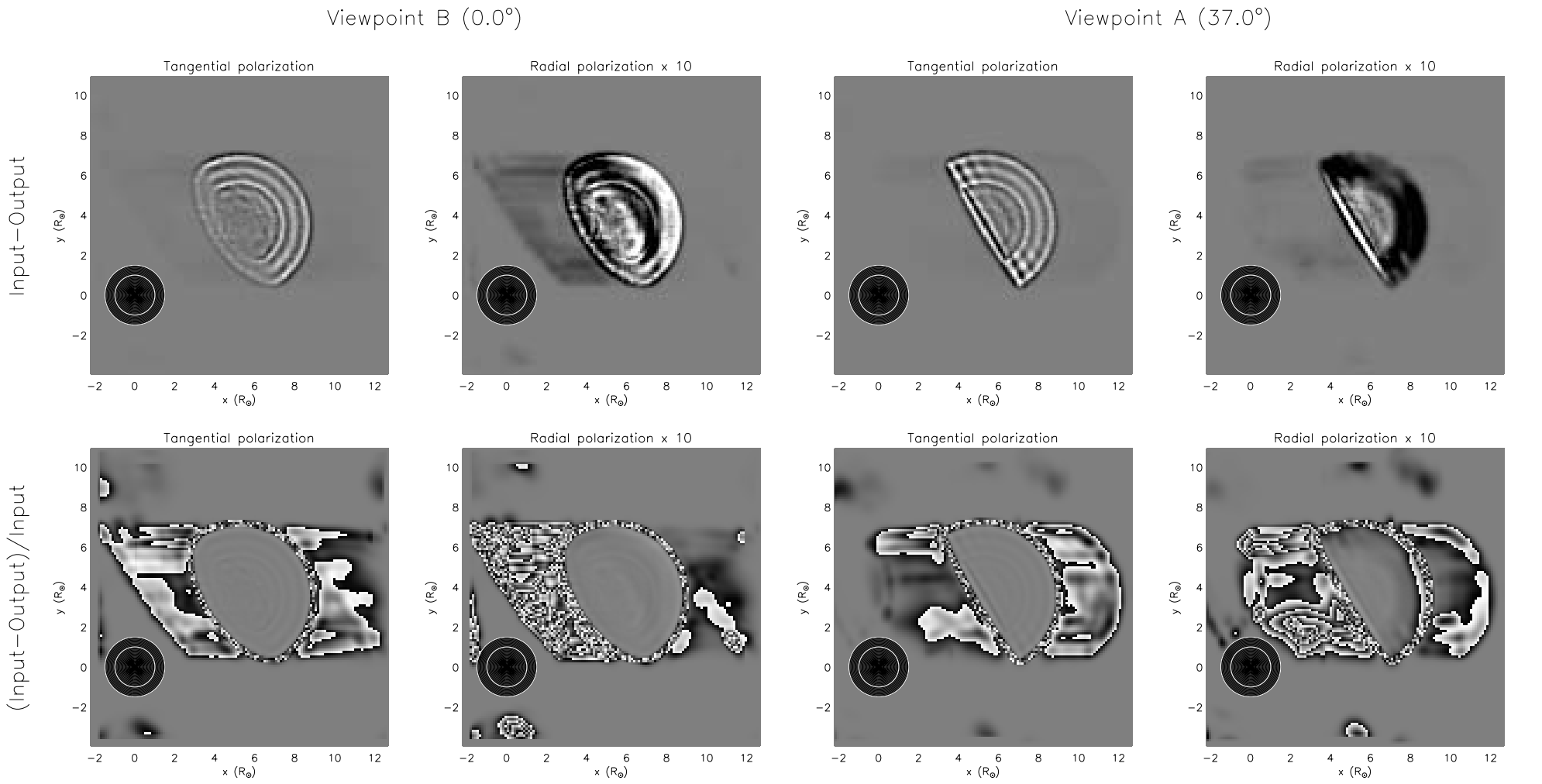

Linear [−6.25e+14, 6.25e+14] photons sec^{-1} cm^{-2} sr^{-1}, No threshold

Fractional error [−2.00, 2.00], Input threshold: 6.25e+12 photons sec^{-1} cm^{-2} sr^{-1}

out_paris__128_05_03b

Figure 5. IMAGEs Visualized from Principal Viewpoints

Column Density, Infinite Geometry

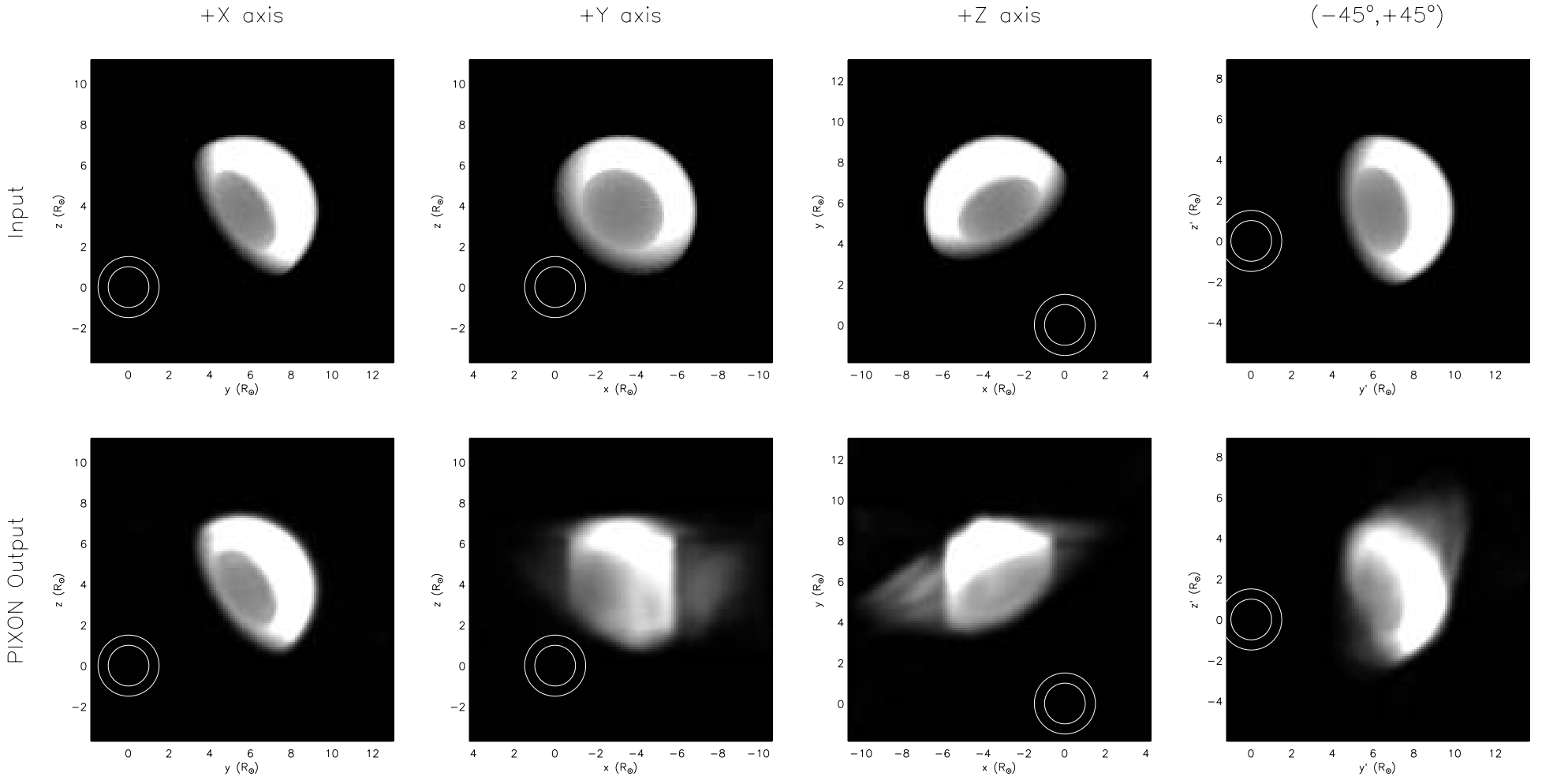

Linear [0, 2.00e+19] electrons cm^{-2}

out_paris__128_05_03b

Figure 7. Histograms of Rendered DATA Above Threshold

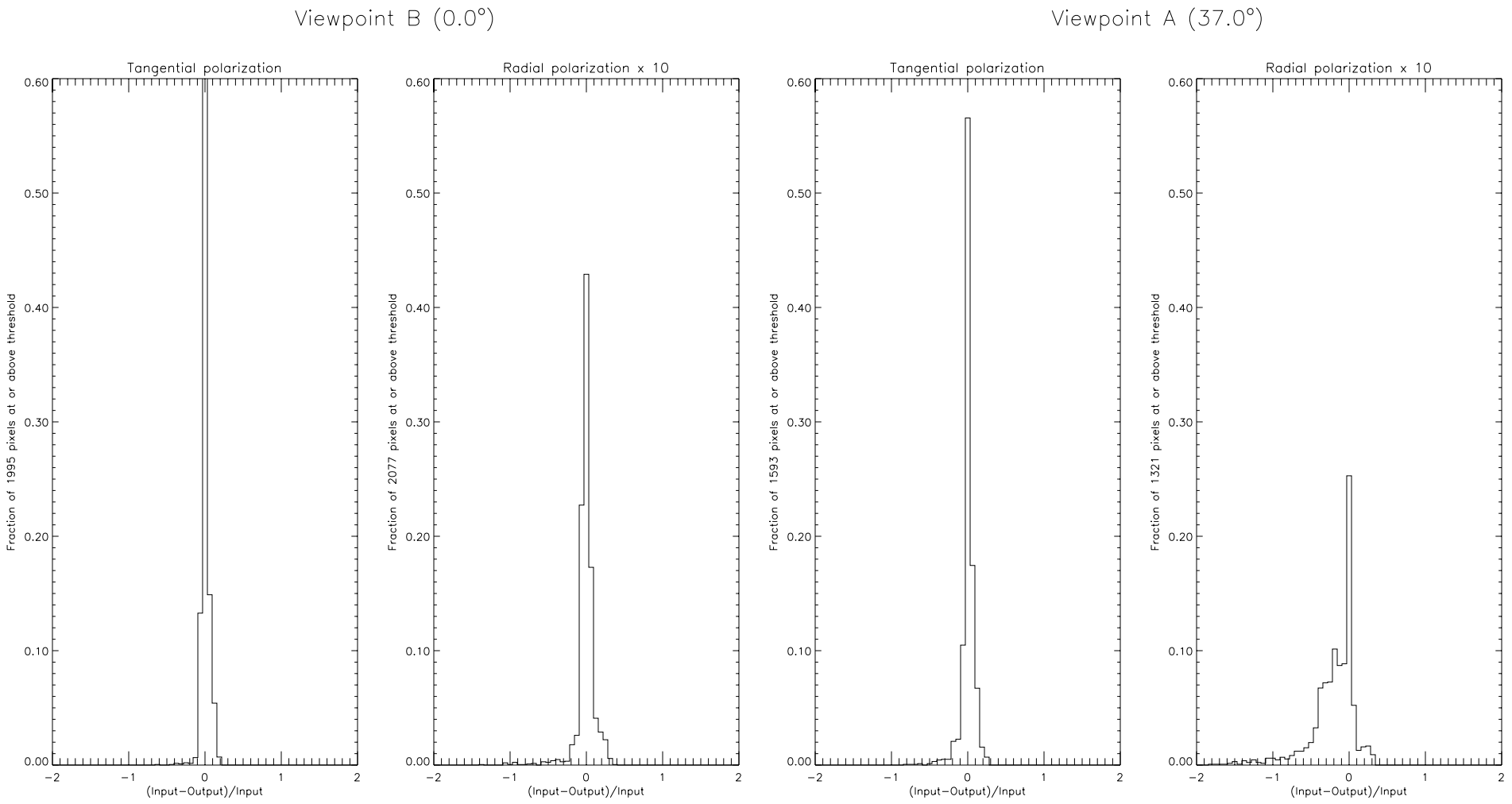

Input Threshold: 6.25e+14 photons sec^{-1} cm^{-2} sr^{-1}

out_paris__128_05_03b

Figure 8. Histograms of IMAGES

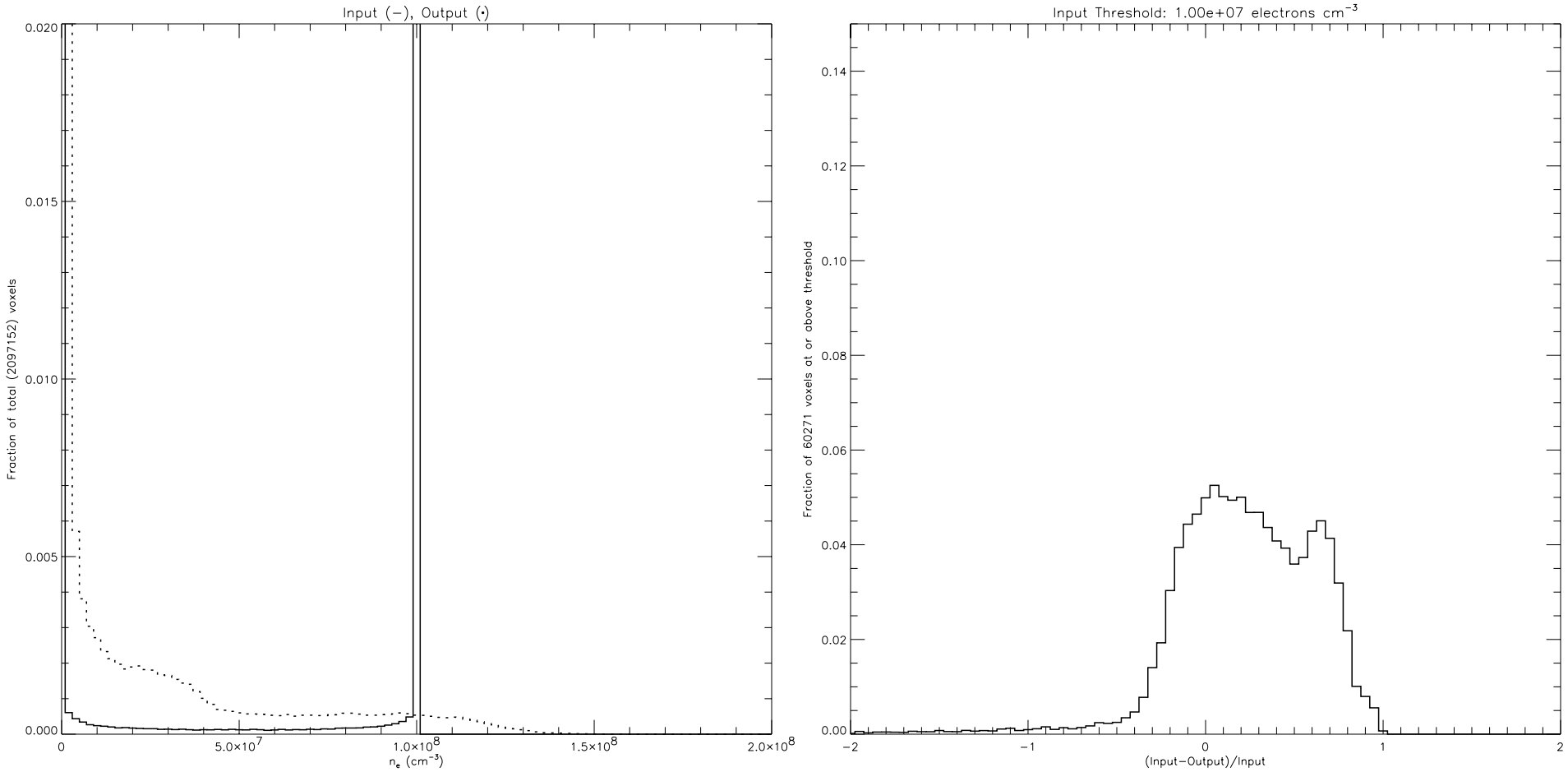

out_paris__128_05_03b